

# Relating Chiral Perturbation Theory and QCD Simulations with Overlap Hypercube Fermions

W. Bietenholz<sup>a</sup> and S. Shcheredin<sup>a,b</sup>  
[for the  $\chi$ LF Collaboration]

<sup>a</sup> Institut für Physik, Humboldt Universität zu Berlin  
Newtonstr. 15, D-12489 Berlin, Germany

<sup>b</sup> Fakultät für Physik, Universität Bielefeld  
D-33615 Bielefeld, Germany

November 21, 2018

## Abstract

We present simulation results for lattice QCD with light pions. For the quark fields we apply chirally symmetric lattice Dirac operators, in particular the overlap hypercube operator, along with the standard overlap operator for comparison. This allows us to simulate at very low pion masses. The results are related to Random Matrix Theory and to Chiral Perturbation Theory in order to extract information about the pion decay constant, the scalar condensate and the topological susceptibility.

## 1 Chiral Perturbation Theory

When a continuous, global symmetry breaks spontaneously, we obtain a continuous set of degenerate vacuum states. Expanding around one selected vacuum, one distinguishes between excitations to higher energy (which are identified with massive particles) and fluctuations, which preserve the ground state energy. The subgroups of the energy conserving symmetry group can either transfer the selected vacuum to a different vacuum state, or leave it simply invariant. The number of generators relating different vacuum states corresponds — according to the Goldstone Theorem — to the number of massless Nambu-Goldstone bosons (NGB) that emerge. At low energy, the NGB can be described by an effective theory as fields in the coset space of the spontaneous symmetry breaking (SSB). Such effective theories still apply if we add a small explicit symmetry breaking; we then deal with light quasi-NGB, which dominate the low energy physics. The effective Lagrangian  $\mathcal{L}_{\text{eff}}$  contains terms of the quasi-NGB fields, which obey the original symmetry, as well as the (explicit) symmetry breaking terms. All these terms are hierarchically ordered according to some low energy counting rules for the momenta and the quasi-NGB masses.

This concept is very general, but it was introduced in the framework of chiral symmetry breaking in QCD. At zero quark masses QCD is assumed

to exhibit a chiral SSB of the form

$$SU(N_f)_L \otimes SU(N_f)_R \rightarrow SU(N_f)_{L+R} , \quad (1)$$

where  $N_f$  is the number of flavours involved. In this case, the coset space is again  $SU(N_f)$ , and the corresponding low energy effective theory is known as *Chiral Perturbation Theory* ( $\chi$ PT) [1].

A small quark mass supplements a slight explicit symmetry breaking, and the quasi-NGB are then identified with the light mesons, i.e. the pions for  $N_f = 2$  — and for  $N_f = 3$  also the kaons and eta particles.

In view of our lattice study, we have to put the system into a finite volume; we choose its shape as  $V = L^3 \times T$  ( $T \geq L$ ). Then  $\chi$ PT was formulated in two regimes, with different counting rules for the terms in  $\mathcal{L}_{\text{eff}}$ . The usual case is characterised by  $Lm_\pi \gg 1$ , where  $m_\pi$  is the pion mass, i.e. the lightest mass involved, which corresponds to the inverse correlation length. This is the *p-regime*, where finite size effects are suppressed, and one expands in the meson momenta and masses (*p-expansion*) [2].

The opposite situation,  $Lm_\pi < 1$ , is denoted as the  *$\epsilon$ -regime*. In that setting, an expansion in the meson momenta is not straightforward, due to the important rôle of the zero modes. Fortunately, the functional integral over these modes can be performed by means of collective variables [3]. There is a large gap to the higher modes, which can then be expanded again, along with the meson masses ( *$\epsilon$ -expansion*) [3, 4].

In both regimes, the leading order of the effective Lagrangian (in Euclidean space) reads

$$\begin{aligned} \mathcal{L}_{\text{eff}} &= \frac{F^2}{4} \text{Tr}[\partial_\mu U^\dagger \partial_\mu U] - \frac{1}{2} \Sigma \text{Tr}[\mathcal{M}(U + U^\dagger)] + \dots , \\ U &\in SU(N_f) , \quad \mathcal{M} = \text{diag}(m_u, m_d, (m_s)) . \end{aligned} \quad (2)$$

The coefficients to these terms are the Low Energy Constants (LEC), and we recognise  $F$  and  $\Sigma$  as the leading LEC. As it stands,  $\Sigma$  and  $F$  occur in the chiral limit  $\mathcal{M} = 0$ ; at realistic light quark masses  $F$  turns into the pion decay constant  $F_\pi$ . Experimentally its value was measured as  $F_\pi \simeq 93$  MeV, which is somewhat above the chiral value of  $F \simeq 86$  MeV [7].  $\Sigma$  is not directly accessible in experiments, but its value is assumed to be  $\gtrsim (250 \text{ MeV})^3$ .

The LEC are of physical importance, but they enter the  $\chi$ PT as free parameters. For a theoretical prediction of their values one has to return to the fundamental theory, which is QCD in this case. There is a notorious lack of analytic tools for QCD at low energy, hence the evaluation of the LEC is a challenge for lattice simulations.

The LEC in nature correspond to their values at  $V = \infty$ , and the *p-regime* is close to this situation. However, it is interesting that these infinite volume values of the LEC can also be determined in the  *$\epsilon$ -regime*, in spite of the strong finite size effects. Actually one makes use exactly of these finite size effects to extract the physical LEC. Generally, we need a long Compton wave length for the pions,  $1/m_\pi$ , and in view of lattice simulations in the *p-regime* we have to use an even much larger box length  $L$ . In this respect, it looks very attractive to work in the  *$\epsilon$ -regime* instead, where we can get away with a small volume.

However, such simulations face conceptual problems: first, light pions can only be realised if the lattice fermion formulation keeps track of the chiral symmetry. In addition, the  *$\epsilon$ -regime* has the peculiarity that the topology plays an important rôle [5]:  $\chi$ PT predictions for expectation

values often refer to distinct topological sectors, so it would be a drastic loss of information to sum them up.

## 2 Lattice QCD with Chiral Fermions

These conceptual problems could be overcome only in the recent years. The solution is the use of a lattice Dirac operator  $D$  which obeys the Ginsparg-Wilson relation [6]. Its simplest form reads (in lattice units)

$$D\gamma_5 + \gamma_5 D = \frac{2}{\mu} D\gamma_5 D, \quad \mu \gtrsim 1, \quad (3)$$

which means that  $D^{-1}$  anti-commutes with  $\gamma_5$ , up to a local term that vanishes in the continuum limit. Even at finite lattice spacing, this local term ( $2\gamma_5/\mu$  in eq. (3)) does not shift the poles in the propagator  $D^{-1}$ . This fermion formulation has a lattice modified, but exact chiral symmetry [8] and exact zero modes with a definite chirality. That property provides a definition of the topological charge by means of the fermionic index  $\nu = n_+ - n_-$  (where  $n_{\pm}$  is the number of zero modes with positive/negative chirality) [9].

The simplest solution to this relation is obtained by inserting the Wilson-Dirac operator  $D_W$  into the so-called overlap formula [10],

$$D_{\text{ov}}^{(0)} = A_{\text{ov}} + \mu, \quad A_{\text{ov}} = \mu A_0 \left( A_0^\dagger A_0 \right)^{-1/2}, \quad A_0 = D_0 - \mu. \quad (4)$$

H. Neuberger suggested this solution with  $D_0 = D_W$ , and we denote the resulting  $D_{\text{ov}}^{(0)}$  as the Neuberger operator (at mass zero). We used it in all our applications presented below at  $\mu = 1.6$ . It is motivated, however, to study also the generalisation with different kernels  $D_0$ , in particular when they already represent an approximate Ginsparg-Wilson operator [11]. We suggested to use a kernel with couplings in a unit hypercube on the lattice (hypercube fermion, HF), which are constructed with Grassmannian block variable renormalisation group transformations [12]. Its gauging also involves “fat links” [13] (the same is also true for the alternative HF kernel of Ref. [14]). Compared to  $D_W$ , multiplications with this kernel require more numerical work (about a factor of 15 in QCD), but part of it is gained back immediately since the evaluation of the overlap operator — which has to be approximated by polynomials in practical implementations — has a faster convergence. There remains an overhead of about a factor 3, but there are further gains of the resulting overlap HF in terms of locality, rotation symmetry and scaling. These virtues have all been tested and confirmed for free fermions [11] and for the 2-flavour Schwinger model [15]. In QCD we worked out such HF kernels at  $\beta = 6/g_0^2 = 6$  [13] and recently also at  $\beta = 5.85$  [16], which corresponds to lattice spacings of  $a \simeq 0.093$  fm resp.  $a \simeq 0.123$  fm (in quenched simulations). Again an improved locality — see Fig. 1 — and rotation symmetry could be confirmed, while a systematic scaling test is still outstanding. The axial anomaly is correctly reproduced in the continuum limit of any topological sector for the Neuberger fermion [18], as well as the overlap HF [19].

A number of subtle numerical tools for simulations with overlap fermions have been elaborated [20], but their simulation is still computationally expensive. For the time being, only quenched QCD simulations are

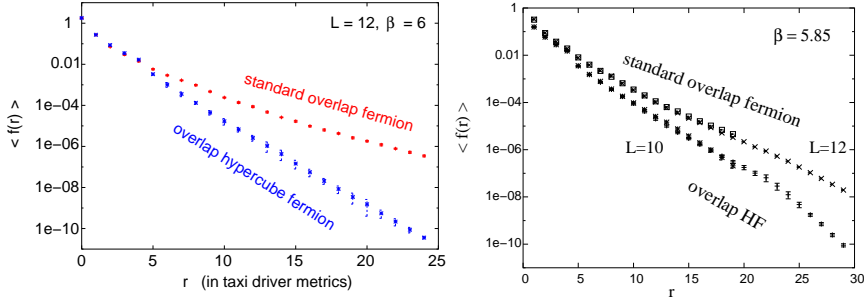


Figure 1: The function  $f(r)$  measures the maximal correlation between sink and source if they are separated by a distance  $r$ . The decay of its expectation value must be (at least) exponential for locality to hold. Our plots show that this is the case for both, the Neuberger fermion [17] and the overlap HF, at  $\beta = 6$  (on the left) and at  $\beta = 5.85$  (on the right) on  $L^4$  lattices. We also see that the decay is clearly faster for the overlap HF, i.e. its locality is significantly improved.

possible; the inclusion of dynamical quarks [21] might be a challenge for the next generation of supercomputers.

In view of the evaluation of Low Energy Constants, the quenched approximation causes logarithmic finite size effects [22]. Nevertheless it is important to explore the potential of this method, in particular in view of the evaluation of LEC in the  $\epsilon$ -regime.

### 3 The Pion Mass

For Wilson's traditional lattice fermion formulation, it was an insurmountable problem to reach light pion masses; due to the additive mass renormalisation and other conceptual problems, the pion masses always remained above about 600 MeV (at least quenched). In order to verify how close we can get to realistic pion masses with the overlap HF, we first evaluate the corresponding pion mass in the  $p$ -regime, as a function of the bare quark mass  $m_q$  (which we assume to be the same for all flavours involved). The latter is added to the chiral operator  $D_{\text{ov}}^{(0)}$  of eq. (4) as

$$D_{\text{ov}}(m_q) = \left(1 - \frac{m_q}{2\mu}\right) D_{\text{ov}}^{(0)} + m_q . \quad (5)$$

The evaluation considers the exponential decay of the pseudoscalar correlation function, which is deformed to a **cosh** behaviour by the periodic boundary conditions. The method can still be improved by subtracting the scalar correlations function, i.e. we study the decays of both,

$$\begin{aligned} C_P(t) &= \sum_{\vec{x}} \langle P^\dagger(\vec{x}, t) P(0) \rangle , \quad \text{and} \\ C_{PS}(t) &= \sum_{\vec{x}} \langle P^\dagger(\vec{x}, t) P(0) - S^\dagger(\vec{x}, t) S(0) \rangle , \end{aligned} \quad (6)$$

where  $P$  and  $S$  are the pseudoscalar and the scalar density. In  $C_{PS}$  some contamination by topological finite size effects is eliminated. The result is shown in Fig. 2 (on the left), which illustrates that the data are in agreement with the expected behaviour  $m_\pi^2 \propto m_q$ . At  $m_q = 0.01$  (in lattice

units) we arrive at a value of  $m_\pi \approx 230$  MeV, i.e. significantly closer to the physical value than the simulations with Wilson fermions. At this point, we are already close to the transition to the  $\epsilon$ -regime,  $m_\pi L \approx 1.7$ . The corresponding pion masses for the Neuberger fermion as measured by our collaboration with more data can be found in Ref. [23]. A measurement in exactly the same way (using the same 29 configurations) based on  $C_P$  is shown for comparison in Fig. 2 on the right.

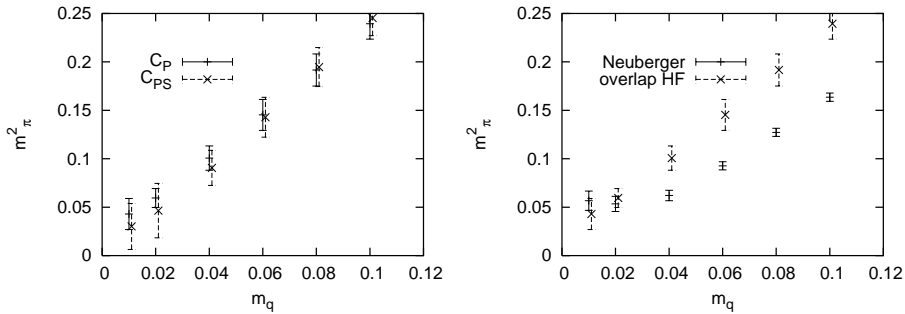


Figure 2: *Left: the pion mass vs. the bare quark mass (both in lattice units) for the overlap HF, evaluated from the temporal decay of the pseudoscalar correlator, with or without subtraction of the scalar correlator. The lowest pion mass in this plot (at  $m_q = 0.01$ ) corresponds to about 230 MeV. This is a preliminary result, based on 29 propagators. On the right we show the comparison to the Neuberger fermion, both evaluated from  $C_P$  in exactly the same way.*

## 4 The Topological Susceptibility

In the quenched approximation, the topological charge (which is identified with the fermion index  $\nu$ ) does not depend on the quark mass. Its statistical distribution is expected to be Gaussian. Fig. 3 (on the left) shows part of our index history for the overlap HF and the Neuberger fermion. They deviate a little,  $|\langle \nu_{\text{ov-HF}} - \nu_N \rangle| \simeq 0.89(4)$ . The plot on the right shows, as an example, our index histogram measured with the Neuberger operator at  $\mu = 1.6$ , which is reasonably consistent with a Gaussian.

From the point of view of the naive, constituent quark model, the  $\eta'$  meson is amazingly heavy ( $m_{\eta'} \simeq 958$  MeV). An explanation for this property was given based on topological windings of the Yang-Mills gauge field. In particular, the Witten-Veneziano formula relates  $m_{\eta'}$  to the topological susceptibility  $\chi_t$  in the leading order of a  $1/N_c$  resp.  $N_f/N_c$  expansion ( $N_c$  is the number of colours),

$$m_{\eta'}^2 = \frac{2N_f}{F_\pi^2} \chi_t, \quad \chi_t = \frac{1}{V} \langle \nu^2 \rangle, \quad \nu : \text{topological charge.} \quad (7)$$

In this formula  $\chi_t$  is understood as a property of pure gauge theory (hence it is sensible to define it with the quenched fermion index), whereas the other terms refer to full QCD. A recent large-scale study with Neuberger fermions [24] arrived in the continuum extrapolation at  $\chi_t = (191 \pm 5 \text{ MeV})^4$ , or — in dimensionless units —  $\chi_t r_0^4 = 0.059(3)$  (where  $r_0$  is the Sommer scale, which translates lattice quantities into physical units). This is consistent with a heavy  $\eta'$  meson.

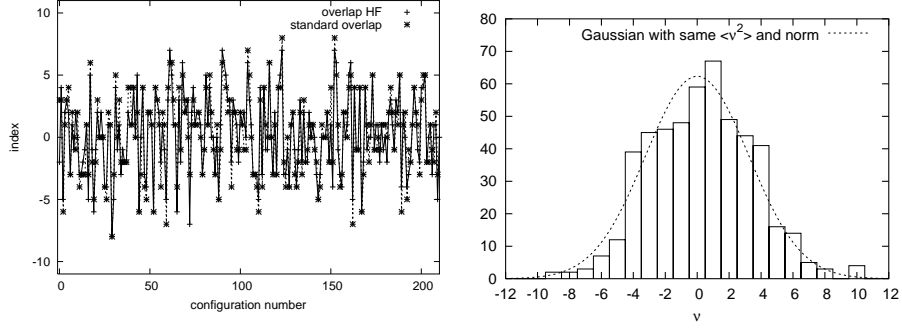


Figure 3: *On the left we show part of the index histories for the overlap HF and the Neuberger fermion, for the same configurations on a  $12^3 \times 24$  lattice at  $\beta = 5.85$ . The plot on the right shows the distribution of topological charges on a  $16^3 \times 32$  lattice at  $\beta = 6$ , measured with the index of the Neuberger operator at  $\mu = 1.6$  on 506 configurations. We see a decent agreement with a Gaussian distribution. Its width represents the topological susceptibility, see Fig. 4.*

In Fig. 4 we show our preliminary result for  $\chi_t r_0^4$  in a physical volume of  $(1.48 \text{ fm})^3 \times 2.96 \text{ fm}$  at lattice spacings  $a = 0.123 \text{ fm}$  and  $a = 0.093 \text{ fm}$ . We include results for the Neuberger operator, as well as the overlap HF, and we also show the continuum extrapolation of Ref. [24] for comparison. Our present data suggest a trend to a somewhat larger value of  $\chi_t r_0^4$ , though the overlap HF is closer to the result of the literature. More statistics will be required to clarify if we arrive at a result consistent with Ref. [24].

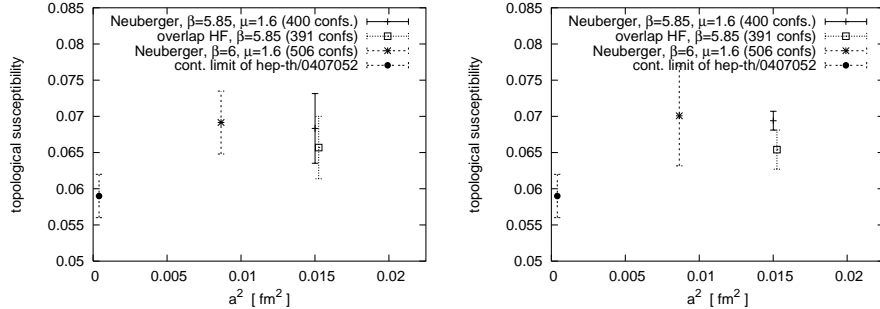


Figure 4: *The topological susceptibility  $\chi_t r_0^4$  at different lattice spacings in the same volume  $V = (1.48 \text{ fm})^3 \times 2.96 \text{ fm}$ . On the left we show our result with the standard statistical evaluation. Alternatively we cut the measured distributions at  $|\nu| = 1.5, 2.5, \dots, 5.5$  and matched them to a Gaussian each time, so that in each case a larger statistics is involved. The results obtained in that way is shown on the right. So far our value for  $\chi_t$  is a little higher than the one of Ref. [24], which is, however, based on a larger statistics.*

## 5 Determination of $\Sigma$

Chiral Random Matrix Theory (RMT) introduces a pseudo Dirac operator

$$D_{\text{RMT}} = \begin{pmatrix} 0 & iW \\ iW^\dagger & 0 \end{pmatrix}, \quad W : \text{complex } n_+ \times n_- \text{ random matrix.} \quad (8)$$

In this way, QCD is simplified to a Gaussian distribution of fermion matrix elements. The hope is to capture nevertheless some properties of QCD in the  $\epsilon$ -regime. In fact, the Leutwyler-Smilga spectral sum rules [5] were successfully reproduced in this way [25].

There are also explicit conjectures for the probability distribution  $\rho$  of the low lying eigenvalues  $i\lambda$  of the continuum Dirac operator. One introduces the dimensionless variable  $z = \lambda\Sigma V$  and considers the spectral density

$$\rho_s(z) = \frac{1}{\Sigma V} \rho\left(\frac{z}{\Sigma V}\right) \Big|_{V=\infty} = \sum_{\nu=-\infty}^{\infty} \rho_s^{(\nu)}(z). \quad (9)$$

Formally this term is taken at  $V = \infty$  (so one deals with a continuous spectrum), although the prediction refers to the  $\epsilon$ -regime. Note, however, that the quark mass is set to zero. This shows that the conjecture involves a number of assumptions, and a test against lattice data is motivated. The last step in eq. (9) is a decomposition into the contributions of the topological sectors, which only depend on  $|\nu|$ . In a fixed sector we can further consider the individual densities of the leading non-zero eigenvalues,

$$\rho_s^{(\nu)}(z) = \sum_{n=1,2,3,\dots} \rho_n^{(\nu)}(z). \quad (10)$$

Chiral RMT provides explicit predictions for the leading densities  $\rho_n^{(\nu)}(z)$  [26], which are supposed to hold up to some energy (depending on the volume). These predictions have been compared to lattice data for overlap fermions in Refs. [27], which did agree for not too small volumes, up to some value of  $z$ .<sup>1</sup> The only free parameter involved in these fits is the scalar condensate  $\Sigma$ . The successful fits provide therefore also a value for  $\Sigma$ , which is found in the range where it is generally expected. At least  $\rho_1^{(\nu)}(z)$  agreed well with the RMT prediction at  $|\nu| = 0, 1, 2$  for  $L \gtrsim 1.1$  fm.

In Fig. 5 we show a new result, for the mean value of the leading non-zero eigenvalue,  $\langle \lambda_1 \rangle$ ,<sup>2</sup> in the topological sectors  $|\nu| = 0, 1, \dots, 5$  on different lattices with different overlap operators, but again in a fixed physical volume. We then fit the RMT predictions for the optimal value of  $\Sigma$  to these data, which yields values in the range  $\Sigma = (268 \text{ MeV})^3 \dots (290 \text{ MeV})^3$ .

At this point we mention that also staggered fermions have a remnant chiral symmetry on the lattice, though not with the full number of generators (in contrast to Ginsparg-Wilson fermions). Thus they are also free of additive mass renormalisation. The standard formulation turned out to be “topology blind”, but a sensitivity to  $|\nu|$  — similar as the one shown in Fig. 5 — can be obtained by a suppression of the mixing between its pseudo-flavours [28].

<sup>1</sup>The work by Giusti et al. is the most extensive study in this context.

<sup>2</sup>The spectrum of our Ginsparg-Wilson operators is actually located on a circle in the complex plane with radius and centre  $\mu$ . For a comparison with the RMT predictions in the continuum, we map this circle with a Möbius transform onto the imaginary axis.

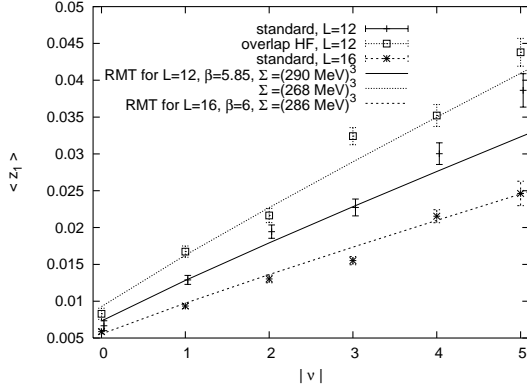


Figure 5: We show our data for the leading non-zero Dirac eigenvalue  $\langle \lambda_1 \rangle$  (resp.  $\langle z_1 \rangle = \Sigma V \langle \lambda_1 \rangle$ ) in the topological sectors  $|\nu| = 0, 1, \dots, 5$ , in a volume  $(1.48 \text{ fm})^3 \times 2.96 \text{ fm}$ . For the Neuberger operator we measured at lattice spacings  $a = 0.093 \text{ fm}$  and  $a = 0.123 \text{ fm}$ , and in the latter case we also used the overlap HF operator. The optimal fit leads to a value for  $\Sigma$  in each case, which is indicated in the plot.

## 6 Mesonic Correlation Functions

To obtain direct predictions for quenched simulations results with chiral lattice fermions, also quenched  $\chi$ PT has been worked out for mesonic correlation functions [29]. The vector correlator vanishes to all orders, and the scalar and pseudoscalar correlators involve additional LEC in the leading order, which are due to quenching. This is not the case for the axial vector correlator, where a parabolic (rather than a `cosh`) behaviour was predicted in the  $\epsilon$ -regime. In fact, this shape could be observed [30] if the spatial box length exceeds about  $L \gtrsim 1.1 \text{ fm}$ , i.e. the same bound that we encountered in Section 5. This also allowed for a determination of  $F_\pi$ . On the other hand, the sensitivity of the curve to  $\Sigma$  is too weak to evaluate it in this way. We further noticed that the Monte Carlo histories in the sector  $\nu = 0$  are plagued by strong spikes, which are related to the significant density of very small Dirac eigenvalues [30] (at higher charges, this density is suppressed). Hence a brute force measurement in the topologically neutral sector would require a tremendous statistics (see also Ref. [31]). A strategy to avoid this problem was proposed and applied in Ref. [32]. Work is also in progress to establish a lattice gauge action, which preserves the topological charge over long periods in the Monte Carlo history [33]. This would help us to measure expectation values in a specific sector — which is desirable in the  $\epsilon$ -regime. With the standard plaquette gauge action (that we are using so far) it is tedious to collect statistics in a specific topology.

Here we turn our attention to another procedure, which only considers the *zero-mode contributions* to the correlators. Following Ref. [34] we focus on the pseudoscalar correlator, where some re-definitions allow us to study only  $F$  and one quenching specific LEC called  $\alpha$  in the leading order of quenched  $\chi$ PT. We distinguish the connected and the disconnected zero-mode contributions,

$$\mathcal{C}_{|\nu|}(x) = \langle v_j^\dagger(x) v_i(x) v_i^\dagger(0) v_j(0) \rangle, \quad \mathcal{D}_{|\nu|}(x) = \langle v_i^\dagger(x) v_i(x) v_j^\dagger(0) v_j(0) \rangle, \quad (11)$$



Dirac operator	$\beta$	lattice size	$ \nu  = 1$	$ \nu  = 2$
Neuberger	5.85	$12^3 \times 24$	95	79
overlap HF	5.85	$12^3 \times 24$	94	83
Neuberger	6	$16^3 \times 32$	115	95

Table 1: *The statistics of configurations at  $|\nu| = 1$  and 2, for different lattices and overlap operators, which was included in our study of the zero-mode contributions to the pseudoscalar correlator. The result is shown in Fig. 6.*

where  $i, j$  are summed over all the zero-modes,  $D_{\text{ov}}^{(0)} v_i = 0$ . It is difficult to fit these quantities directly, but it is easier to fit the data to the leading order in the expansion around the minimum in the time coordinate  $t$  [34] (after summation over the spatial lattice sites  $\vec{x}$ ). This minimum is at  $T/2$ , hence we expand in  $s = t - T/2$ ,

$$\frac{1}{L^2} \frac{d}{ds} \mathcal{C}_{|\nu|}(s) \simeq \frac{s}{T} \cdot \tilde{\mathcal{C}}_{|\nu|}, \quad \frac{1}{L^2} \frac{d}{ds} \mathcal{D}_{|\nu|}(s) \simeq \frac{s}{T} \cdot \tilde{\mathcal{D}}_{|\nu|}, \quad (12)$$

where we neglect  $\mathcal{O}((s/T)^3)$ . The combined fit of our data in the sectors  $|\nu| = 1, 2$  to  $\tilde{\mathcal{C}}$  and  $\tilde{\mathcal{D}}$  — at different values of  $s$  — leads to the results for  $F$  and  $\alpha$  shown in Fig. 6 [16], see also Ref. [35]. (In these fits we also made use of our measured results for  $\langle \nu^2 \rangle$ .) Since eqs. (12) only hold up to  $\mathcal{O}((s/T)^3)$  we should extrapolate down to small  $s$ . We only obtained a stable extrapolation, with acceptable errors, for the overlap HF, but not for the Neuberger operator on two different lattice spacings — although the statistics is similar, see Table 1.

The result of these extrapolations agrees within the (sizable) errors with Ref. [34]. Note that these are values for the bare parameters. In particular the renormalisation of  $F$  involves the factor  $Z_A$ , which amounts to about 1.45 in the chiral limit for our parameters of the Neuberger operator at  $\beta = 5.85$  [23].

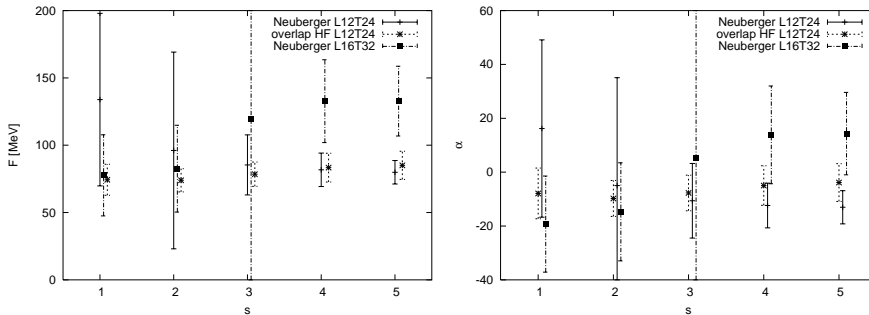


Figure 6: *Results for  $F$  and  $\alpha$  (LEC in the leading order of quenched  $\chi$ PT), based on our data for the zero-mode contribution to the pseudo-scalar correlation function in the topological sectors  $|\nu| = 1$  and 2. In both cases, we obtain a stable behaviour and a decent extrapolation down to a small fitting range  $s$  only for the overlap HF. The statistics for these plots is given in Table 1.*

## 7 Conclusions

We discussed the potential of relating simulation results for lattice QCD with chiral fermions to the predictions by  $\chi$ PT. For the first time we applied the overlap HF in this context and compared its results also with Neuberger's standard overlap operator. We gave preliminary results for the pion mass in the  $p$ -regime. In the  $\epsilon$ -regime we are interested in the determination of the LEC that appear in the effective Lagrangian.

This project is still on-going, as part of the efforts of the  $\chi$ LF collaboration to simulate QCD close to the chiral limit. For the approach discussed here we saw that we can go down close to 200 MeV with the pion mass. The evaluation of the LEC in the leading order seems feasible, though a larger statistics is required for this purpose. So far we can report that data obtained in the  $\epsilon$ -regime — i.e. in small volumes — can indeed be matched with the analytical predictions by chiral RMT and quenched  $\chi$ PT. We expect the same property also for dynamical chiral quarks, once our machines are powerful enough to simulate them.

**Acknowledgement** *We are indebted to the whole  $\chi$ LF collaboration for its cooperation, in particular to Mauro Papinutto and Carsten Urbach for providing us with highly optimised eigenvalue routines, and to Kei-ichi Nagai for contributing to the zero-mode study in an early stage. W.B. thanks the organisers of the Titeica-Markov Symposium for their kind hospitality. This work was supported by the Deutsche Forschungsgemeinschaft through SFB/TR9-03. The computations were performed on the IBM p690 clusters of the "Norddeutscher Verbund für Hoch- und Höchstleistungsrechnen" (HLRN) and at NIC, Forschungszentrum Jülich. Finally we thank Hinnerk Stüben for his advice on the parallelisation of our codes.*

## References

- [1] S. Weinberg, *Physica* **A96** (1979) 327. J. Gasser and H. Leutwyler, *Ann. Phys. (N.Y.)* **158** (1984) 142.
- [2] J. Gasser and H. Leutwyler, *Phys. Lett.* **B184** (1987) 83.
- [3] J. Gasser and H. Leutwyler, *Phys. Lett.* **B188** (1987) 477.
- [4] H. Neuberger, *Phys. Rev. Lett.* **60** (1988) 889; *Nucl. Phys.* **B300** (1988) 180. P. Hasenfratz and H. Leutwyler, *Nucl. Phys.* **B343** (1990) 241. F.C. Hansen, *Nucl. Phys.* **B345** (1990) 685. F.C. Hansen and H. Leutwyler, *Nucl. Phys.* **B350** (1991) 201. W. Bietenholz, *Helv. Phys. Acta* **66** (1993) 633.
- [5] H. Leutwyler and A. Smilga, *Phys. Rev.* **D46** (1992) 5607.
- [6] P.H. Ginsparg and K.G. Wilson, *Phys. Rev.* **D25** (1982) 2649.
- [7] G. Colangelo and S. Dürr, *Eur. Phys. J.* **C33** (2004) 543.
- [8] M. Lüscher, *Phys. Lett.* **B428** (1998) 342.
- [9] P. Hasenfratz, V. Laliena and F. Niedermayer, *Phys. Lett.* **B427** (1998) 317. P. Hasenfratz, *Nucl. Phys.* **B525** (1998) 401.
- [10] H. Neuberger, *Phys. Lett.* **B417** (1998) 141.
- [11] W. Bietenholz, *Eur. Phys. J.* **C6** (1999) 537.
- [12] U.-J. Wiese, *Phys. Lett.* **B315** (1993) 417. W. Bietenholz and U.-J. Wiese, *Phys. Lett.* **B378** (1996) 222; *Nucl. Phys.* **B464** (1996) 319. W. Bietenholz, R. Brower, S. Chandrasekharan and U.-J. Wiese, *Nucl. Phys. (Proc. Suppl.)* **B53** (1997) 921.

- [13] W. Bietenholz, *Nucl. Phys.* **B644** (2002) 223.
- [14] P. Hasenfratz, S. Hauswirth, T. Jörg, F. Niedermayer and K. Holland, *Nucl. Phys.* **B643** (2002) 280.
- [15] W. Bietenholz and I. Hip, *Nucl. Phys.* **B570** (2000) 423.
- [16] S. Shcheredin, Ph.D. thesis, Berlin (2004) [[hep-lat/0502001](#)].
- [17] P. Hernández, K. Jansen and M. Lüscher, *Nucl. Phys.* **B552** (1999) 363.
- [18] D.H. Adams, *Annals Phys.* **296** (2002) 131.
- [19] D.H. Adams and W. Bietenholz, *Eur. Phys. J.* **C34** (2004) 245.
- [20] J. van den Eshof, A. Frommer, Th. Lippert, K. Schilling, H.A. van der Vorst, *Comput. Phys. Commun.* **146** (2002) 203. L. Giusti, C. Hoelbling, M. Lüscher and H. Wittig, *Comput. Phys. Commun.* **153** (2003) 31. G. Arnold *et al.*, [hep-lat/0311025](#). N. Cundy *et al.*, [hep-lat/0405003](#). T. Chiarappa *et al.*, [hep-lat/0409107](#).
- [21] Z. Fodor, S.D. Katz and K.K. Szabo, *JHEP* **0408** (2004) 003. N. Cundy *et al.*, [hep-lat/0409029](#), [hep-lat/0502007](#). T. DeGrand and S. Schaefer, [hep-lat/0412005](#).
- [22] P.H. Damgaard, *Phys. Lett.* **B608** (2001) 162.
- [23]  $\chi$ LF collaboration, *JHEP* **0412** (2004) 044.
- [24] L. Del Debbio, L. Giusti and C. Pica, [hep-th/0407052](#).
- [25] J.J.M. Verbaarschot and I. Zahed, *Phys. Rev. Lett.* **70** (1993) 3852.
- [26] P.H. Damgaard and S.M. Nishigaki, *Nucl. Phys.* **B518** (1998) 495; *Phys. Rev.* **D63** (2001) 045012. T. Wilke, T. Guhr and T. Wettig, *Phys. Rev.* **D57** (1998) 6486. S.M. Nishigaki, P.H. Damgaard and T. Wettig, *Phys. Rev.* **D58** (1998) 087704.
- [27] W. Bietenholz, K. Jansen and S. Shcheredin, *JHEP* **07** (2003) 033. L. Giusti, M. Lüscher, P. Weisz and H. Wittig, *JHEP* **11** (2003) 023. D. Galletly *et al.*, *Nucl. Phys. (Proc. Suppl.)* **B129/130** (2004) 456.
- [28] S. Dürr and C. Hoelbling, *Phys. Rev.* **D69** (2004) 034503. E. Follana, A. Hart and C.T.H. Davies, *Phys. Rev. Lett.* **93** (2004) 241601. S. Dürr, C. Hoelbling and U. Wenger, *Phys. Rev.* **D70** (2004) 094502. Kit Yan Wong and R.M. Woloshyn, [hep-lat/0412001](#).
- [29] P.H. Damgaard *et al.*, *Nucl. Phys.* **B629** (2002) 226; *Nucl. Phys.* **B656** (2003) 226.
- [30] W. Bietenholz, T. Chiarappa, K. Jansen, K.-I. Nagai and S. Shcheredin, *JHEP* **02** (2004) 023.
- [31] P. Hernández, K. Jansen and L. Lellouch, *Phys. Lett.* **B469** (1999) 198.
- [32] L. Giusti, P. Hernández, M. Laine, P. Weisz and H. Wittig, *JHEP* **0404** (2004) 013.
- [33] H. Fukaya and T. Onogi, *Phys. Rev.* **D68** (2003) 074503; *Phys. Rev.* **D70** (2004) 054508. S. Shcheredin, W. Bietenholz, K. Jansen, K.-I. Nagai, S. Necco, and L. Scorzato, [hep-lat/0409073](#). W. Bietenholz, K. Jansen, K.-I. Nagai, S. Necco, L. Scorzato and S. Shcheredin, [hep-lat/0412017](#).
- [34] L. Giusti, P. Hernández, M. Laine, P. Weisz and H. Wittig, *JHEP* **0401** (2004) 003.
- [35] K.-I. Nagai, *unpublished notes*.